

Axions on a Hyperbolic Ride: Geometric Suppression of CMB Isocurvature and a Blue-Tilted Spectrum

Sai Chaitanya Tadepalli*

Physics Department, Indiana University, Bloomington, IN 47405, USA

CMB limits on cold-dark-matter isocurvature are often interpreted as excluding the simultaneous realization of high-scale inflation and large QCD axion decay constants in pre-inflationary Peccei–Quinn (PQ) scenarios. This conclusion can be evaded by exploiting *field-space geometry*. For a minimal complex PQ scalar with a $U(1)$ -symmetric potential and a nonlinear sigma-model kinetic term $d\sigma^2 = dR^2 + f^2(R) d\theta^2$, the observable axion fluctuation is $\delta\theta \sim H_{\text{inf}}/f(R)$, so an enhanced effective decay constant $f(R)$ suppresses isocurvature without explicit PQ breaking, extreme radial displacements, or additional couplings. We specialize to a hyperbolic metric $f(R) \propto \sinh(R/L)$ with curvature scale L . The same geometry also induces a time-dependent $\mathcal{O}(H_{\text{inf}})$ effective mass for the canonical axial mode during radial slow-roll, and fixing the tilt and running of isocurvature. Thus, CMB-scale isocurvature is suppressed while a characteristic blue-tilted spectrum is generated. As a result, inflationary Hubble scales as large as $H_{\text{inf}} \sim 10^{13}$ GeV can be compatible with $f_a \sim 10^{14}$ – 10^{16} GeV, reopening parameter space usually regarded as excluded. We present ‘observable’ benchmarks and a semi-analytic template that relates the scale-dependence of isocurvature to the geometric lever arm R/L , providing a direct phenomenological probe on PQ field-space geometry.

I. INTRODUCTION

The QCD axion provides a dynamical solution to the strong–CP problem and is a well-motivated dark matter (DM) candidate [1–10]. In the pre-inflationary PQ-breaking scenario, inflation homogenizes the axion field over our observable patch, leaving a coherent background misalignment angle θ_i . However, quantum fluctuations generated during inflation persist as cold-dark-matter isocurvature perturbations, while the axion density also carries the usual adiabatic mode inherited from the primordial curvature perturbation. Current CMB limits on the isocurvature fraction in [11–13] therefore translate into a stringent constraint on high-scale inflation as a function of (f_a, θ_i) , sharply disfavoring a vast regime of large axion decay constant f_a (e.g. near the GUT scale) together with $H_{\text{inf}} \sim 10^{13}$ GeV [14].

The axion isocurvature bound has motivated three main classes of proposals. (i) *Heavy axion during inflation*: suppress fluctuations by making the angular mode heavy, $m_a \gtrsim H_{\text{inf}}$, so that superhorizon perturbations are exponentially damped. This can come from a temporarily modified axion potential (enhanced QCD during inflation [15–18], curvature/higher-dimensional terms [19], monodromy/BF-type masses [20]) or SUSY/multi-field transitions that leave a light QCD axion only later [21]. Such mechanisms often require explicit PQ-breaking during inflation and satisfying axion-quality/strong–CP alignment at late times [22, 23]. (ii) *Large effective decay constant*: suppress fluctuations by displacing the radial field (R) so that $R \gg f_a$, and hence the spectrum is suppressed by $(H_{\text{inf}}/(R\theta_i))^2$ [21, 24–32]. In the minimal quartic PQ model this tends to force tiny quartic coefficient λ , large excursions (EFT sensitiv-

ity), and complicated post-inflationary dynamics (resonance/fragmentation), with the highest- H_{inf} regime especially delicate [33]. (iii) *Blue-tilted isocurvature*: use out-of-equilibrium PQ dynamics so the rolling (or rotating) radial background induces a time-dependent mass for angular fluctuations, suppressing CMB modes while enhancing smaller scales [34, 35]. Achieving large blue-tilted spectra over a long range of scales are easiest with effectively quadratic radial evolution (e.g. Hubble masses). However, pure quartic potential typically yield only a short range unless additional dynamics (e.g. sustained rotation) is present [36].

In this work we present a minimal, $U(1)$ conserving alternative based on field-space geometry. Curved internal field-space metrics are well known to generate effective masses and characteristic scale-dependence for entropic/isocurvature modes in covariant sigma-model systems [37–42]. In this *Letter*, we apply this mechanism to the QCD axion, modeled by a minimal PQ complex scalar field with a quartic potential and a spontaneously broken $U(1)_{\text{PQ}}$. A hyperbolic field-space metric then exponentially suppresses the observable angular fluctuation without explicit PQ breaking, while the evolving axion mass produces a distinctive blue-tilted isocurvature spectrum on smaller scales. As a result, viable parameter space with $H_{\text{inf}} \sim 10^{13}$ GeV and large f_a (e.g. $\lesssim 10^{16}$ GeV) can be reopened without requiring the extreme displacements $R_{\text{inf}}/f_a \sim 10^4$ – 10^5 or tiny quartic coefficients $\lesssim \mathcal{O}(10^{-16})$. The effective radial mass and the geometric lever arm control the ‘detectability’ of these isocurvatures. Thus, we further provide a compact phenomenological template relating the isocurvature spectral index to the field-space curvature scale, thereby promoting measurements of isocurvature scale-dependence to a direct probe of PQ field-space geometry.

The paper is organized as follows. Section II reviews the axion isocurvature constraint, Sec. III introduces the hyperbolic PQ field-space framework, and Sec. IV

* saictade@iu.edu

presents benchmarks and resulting spectra. We conclude in Sec. V. Appendices A and B give a UV-motivated origin for the hyperbolic metric, and a semi-analytic data-facing template respectively.

II. THE STANDARD QCD AXION ISOCURVATURE PROBLEM

In the pre-inflationary PQ scenario, if the axion field ($a(x) = f_{\text{eff}}\theta(x)$) is light during inflation, its superhorizon fluctuations are set by the de Sitter result

$$\delta a \simeq \frac{H_{\text{inf}}}{2\pi}, \quad \delta\theta \simeq \frac{\delta a}{f_{\text{eff}}(t_*)}, \quad (1)$$

where $f_{\text{eff}}(t_*)$ is the effective decay constant at CMB horizon exit (typically $f_{\text{eff}} = f_a$ in minimal models), and θ_i is the misalignment angle. See [5] for a review of the discussion in this section.

In the harmonic regime $|\theta_i| \lesssim 1$, the axion density scales as $\rho_a \propto \theta_i^2$, so the isocurvature mode is

$$S_a \simeq \frac{\delta\rho_a}{\rho_a} \simeq 2 \frac{\delta\theta}{\theta_i}. \quad (2)$$

If axions constitute a fraction $r_a \equiv \Omega_a/\Omega_{\text{DM}}$ of the total DM, then the matter isocurvature power is

$$\Delta_S^2(k) \simeq 4r_a^2 \frac{\Delta_\theta^2(k)}{\theta_i^2} \simeq 4r_a^2 \frac{H_{\text{inf}}^2}{(2\pi)^2 f_{\text{eff}}^2(t_*) \theta_i^2}, \quad (3)$$

which is approximately scale invariant in the light-axion limit. CMB data constrain the isocurvature fraction at the percent level near the pivot $k_* = 0.002 \text{ Mpc}^{-1}$, implying (for $r_a \simeq 1$ and $f_{\text{eff}} = f_a$)

$$\frac{H_{\text{inf}}}{f_a \theta_i} < 2.8 \times 10^{-5}. \quad (4)$$

For QCD axions making all of DM via misalignment in a standard thermal history, θ_i is fixed by f_a through the relic abundance. Using the usual scaling $\Omega_a \propto f_a^{7/6} \theta_i^2$ (up to $\mathcal{O}(1)$ uncertainties), $\Omega_a = \Omega_{\text{DM}}$ gives ([6, 43])

$$\theta_i \equiv \theta_{i,\text{QCD}} \simeq \left(\frac{7.4 \times 10^{11} \text{ GeV}}{f_a} \right)^{7/12}. \quad (5)$$

This relation assumes the PQ radial field has relaxed to its late-time vacuum well before the QCD epoch, so the decay constant at the onset of oscillations is f_a .

Fig. 1 displays the resulting tension in the (H_{inf}, f_a) plane for the usual QCD axion. If the inflationary effective decay constant is enhanced to $f_{\text{eff}} = \kappa f_a$, the bound is relaxed accordingly. $T_{\text{inst,RH}}$ is the instantaneous reheating temperature and the orange solid line marks the upper boundary of the region for PQ restoration post-inflation. In flat-metric PQ models, realizing simultaneously $H_{\text{inf}} \simeq 10^{13} \text{ GeV}$ and $f_a \sim 10^{16} \text{ GeV}$ typically forces $\kappa \gtrsim 10^4$, often into a regime where the spectator/EFT description is difficult to control.

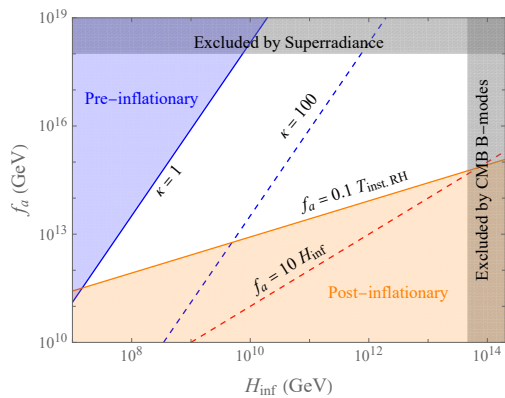


FIG. 1. Illustrative constraints in the (H_{inf}, f_a) plane for pre-inflationary QCD axion DM from misalignment. For the standard flat-metric case $f_{\text{eff}} = f_a$, the isocurvature bound restricts QCD axion to the blue shaded region. Gray bands indicate additional excluded regions. We focus on how the white region can be reopened using geometric suppression. (Redrawn with inspiration from [33].)

III. HYPERBOLIC PQ FIELD-SPACE AND GEOMETRIC SUPPRESSION

During inflation we take a quasi-de Sitter background with spatially flat FRW metric

$$ds^2 = -dt^2 + a(t)^2 dx^2, \quad a(t) \simeq e^{Ht}, \quad (6)$$

where $H \simeq H_{\text{inf}}$ is approximately constant. We consider a spectator PQ complex scalar Φ with a $U(1)$ -symmetric potential and allow a nontrivial internal field-space metric. Writing

$$\Phi(x) = \frac{R(x)}{\sqrt{2}} e^{i\theta(x)}, \quad (7)$$

we adopt the diagonal sigma-model form

$$d\sigma^2 = dR^2 + f^2(R) d\theta^2, \quad (8)$$

so that the action can be written as

$$S = \int d^4x \sqrt{-g} \left[-\frac{1}{2} (\partial R)^2 - \frac{1}{2} f^2(R) (\partial\theta)^2 - V(R) \right], \quad (9)$$

with $f^2(R) > 0$ and no explicit θ -dependence in V .

See Supplemental Material at [44] for derivations in this section. We work in the vanishing-charge background $\dot{\theta}_0 = 0$, for which the homogeneous evolution is purely radial,

$$\ddot{R}_0 + 3H\dot{R}_0 + V_{,R}(R_0) = 0, \quad (10)$$

and is independent of $f(R)$. The effect of the curved metric appears in the fluctuations. The radial perturbation obeys

$$\delta\ddot{R} + 3H\delta\dot{R} - \frac{\nabla^2}{a^2} \delta R + V_{,RR}(R_0) \delta R = 0. \quad (11)$$

Defining the canonically normalized angular fluctuation $\delta\psi \equiv f(R_0)\delta\theta$, one finds

$$\ddot{\delta\psi} + 3H\dot{\delta\psi} - \frac{\nabla^2}{a^2}\delta\psi + m_\psi^2(t)\delta\psi = 0, \quad (12)$$

with the time-dependent effective mass

$$m_\psi^2(t) = \frac{f'}{f}V_{,R}(R_0) - \frac{f''}{f}\dot{R}_0^2, \quad (13)$$

(primes denote derivatives with respect to R , evaluated on $R_0(t)$). In flat field-space ($f(R) = R$) one recovers $m_\psi^2 \simeq V_{,R}/R_0$, so the axial fluctuation has a mass of the same order as the radial mode, and the two evolve with comparable effective masses.

Hyperbolic metric. We instead consider a constant negative-curvature field-space,

$$d\sigma^2 = dR^2 + L^2 \sinh^2\left(\frac{R}{L}\right) d\theta^2, \quad f(R) = L \sinh\left(\frac{R}{L}\right), \quad (14)$$

with curvature scale $L > 0$. See Appendix A for a UV-motivated example that realizes this metric through a Kähler manifold. Then

$$m_\psi^2(t) = \frac{1}{L} \coth\left(\frac{R_0}{L}\right) V_{,R}(R_0) - \frac{1}{L^2} \dot{R}_0^2. \quad (15)$$

For $R_0 \gtrsim L$ and slow-roll background radial evolution, it is useful to write

$$m_\psi^2(t) \approx H_{\text{inf}}^2 \left(\delta - \frac{\delta^2}{9} \right), \quad (16)$$

where

$$\delta \equiv \xi \frac{m_R^2}{H_{\text{inf}}^2}, \quad \xi \equiv \frac{R_0}{L}, \quad m_R^2 \equiv \frac{V_{,R}(R_0)}{R_0}. \quad (17)$$

The leading geometric contribution is enhanced by the curvature lever arm $\xi = R_0/L$, while the subleading negative term encodes the reduction of transverse masses from negative curvature when $\dot{R}_0 \neq 0$. Unlike for a flat-metric, the axial mode can become $\mathcal{O}(H)$ -heavy even during radial slow-roll. The time dependence generically produces blue-tilted isocurvature: modes exiting earlier (larger scales) are most suppressed, while later-exiting modes (smaller scales) are less suppressed. From Eq. (15), we also note that large radial velocities (underdamped motion) tend to destabilize the angular mode.

IV. BENCHMARK MODELS AND ISOCURVATURE SPECTRUM

We adopt the minimal quartic PQ potential

$$V(R) = \frac{\lambda}{4} (R^2 - f_{\text{PQ}}^2)^2, \quad f_{\text{PQ}} \simeq f_a, \quad (18)$$

with hyperbolic metric Eq. (14) and work in the vanishing charge sector $\dot{\theta}_0 = 0$. We evolve the background

fields during inflation, using $N \equiv \ln a$, and compute fluctuations mode-by-mode with Bunch-Davies initial conditions deep inside the horizon. The angular power spectrum is

$$\Delta_\theta^2(k) \equiv \frac{k^3}{2\pi^2} |\delta\theta_k|^2, \quad \delta\theta_k = \frac{\delta\psi_k}{f(R_0)} \Big|_{\text{late-time}}. \quad (19)$$

In the harmonic regime, the total matter isocurvature spectrum is given by Eq. (3) evaluated at the end of inflation N_{inf} . For QCD axion DM from misalignment, we eliminate θ_i using Eq. (5).

	λ	f_a/H_{inf}	R_i/H_{inf}	N_{inf}	L/H_{inf}
B1	2×10^{-7}	10^1	1.5×10^3	55	1.1×10^2
B2	4×10^{-6}	10^1	3.5×10^2	55	2.1×10^1
B3	2×10^{-9}	10^3	1.5×10^4	55	1.1×10^3

TABLE I. Benchmark parameter choices.

We consider three benchmark points B1-B3 (Tab. I), chosen such that the initial curvature lever arm $\xi_i \equiv R_i/L$ is $\sim \mathcal{O}(10)$ and CMB-scale isocurvature is evaluated at a high $H_{\text{inf}} \sim 10^{13}$ GeV. The near-degeneracy of B1 and B3 is intentional: in H_{inf} units the spectator PQ system has an approximate rescaling symmetry,

$$R \rightarrow \frac{R}{x}, \quad L \rightarrow \frac{L}{x}, \quad f_a \rightarrow \frac{f_a}{x^{24/14}}, \quad \lambda \rightarrow \lambda x^2, \quad (20)$$

which leaves the dimensionless geometry (R/L) and the radial mass in Hubble units approximately invariant, yielding nearly identical spectra for B1 and B3 despite different f_a . Benchmark B2 instead illustrates the breadth of viable parameter space at fixed $f_a/H_{\text{inf}} = 10$ by varying ($\lambda, R_i/L, L/H_{\text{inf}}$).

A. Results

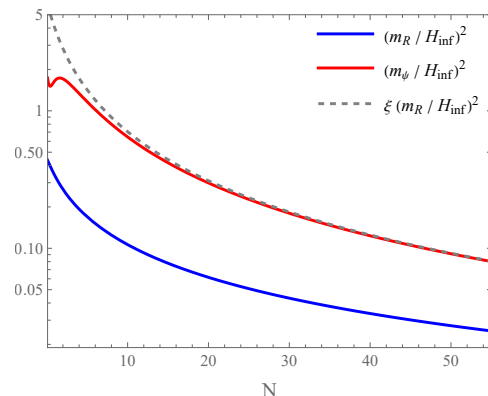


FIG. 2. Time-dependent mass-squared of the angular fluctuation (m_ψ^2) and background radial mass-scale (m_R^2) for B1.

Fig. 2 shows the mass history for B1. The radial field slow-rolls toward its vacuum, while the hyperbolic

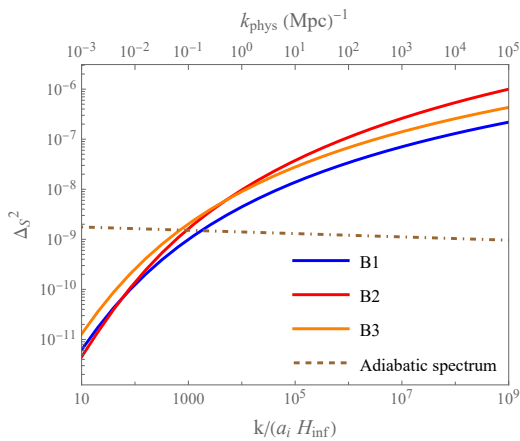


FIG. 3. Total matter isocurvature spectra for the benchmarks, assuming QCD axions constitute all DM via misalignment ($r_a = 1$). We take $H_{\text{inf}} = 10^{13}$ GeV. Adiabatic spectrum also shown for $A_s = 2.1 \times 10^{-9}$ and $n_s = 0.967$ [12].

metric induces a geometric axial mass. Initially $m_R^2 \lesssim \mathcal{O}(0.1)H_{\text{inf}}^2$ while $m_\psi^2 \sim \mathcal{O}(H_{\text{inf}}^2)$, so modes exiting early are damped. As R_0 decreases and \dot{R}_0 redshifts, $m_\psi^2/H_{\text{inf}}^2$ falls and the damping weakens for later-exiting modes. In the regime $\delta = \xi(m_R/H_{\text{inf}})^2 \lesssim 1$, the dominant behavior is $m_\psi^2 \simeq \xi m_R^2$, i.e. the angular mode is enhanced relative to the flat case by the curvature lever arm $\xi = R/L$, while for $\xi m_R^2 \gtrsim 1$ the negative curvature term $\propto -\dot{R}^2$ reduces the effective axial mass.

Fig. 3 shows the resulting conserved superhorizon $\Delta_S^2(k)$. We take $k/(a_i H_{\text{inf}}) = 10$ to correspond to the CMB pivot scale $k_* \simeq 0.002, \text{Mpc}^{-1}$. Power is strongly suppressed on the largest CMB scales because those modes exit while $f(R)$ is exponentially enhanced, so that the observable fluctuation $\delta\theta = \delta\psi/f(R)$ is strongly suppressed at horizon exit [42]. As R slow-rolls during the radial evolution, $f(R(t_k))$ decreases and smaller scales are progressively less suppressed. The outcome is a blue-tilted isocurvature spectrum with running over the range of modes that probe the evolution of R , approaching a quasi-plateau once the angular mode becomes light. Equivalently and rather more accurately, this behavior can be described in terms of the time-dependent effective mass $m_\psi^2(t)$ during radial slow-roll, which governs evolution of $\delta\psi$ while leaving the ratio $\delta\psi/f(R) = \delta\theta$ nearly conserved in the slow-roll regime outside the horizon.

B. Detectability of isocurvature signal

For $R/L \gg 1$, the hyperbolic metric implies $\Delta_\theta^2 \sim (H_{\text{inf}}/L)^2 e^{-2R/L}$, so that for $R/L \gg 10$, the isocurvature amplitude is negligible and phenomenologically irrelevant. For representative values $H_{\text{inf}} \lesssim L$, near-term observability therefore requires $R \lesssim \mathcal{O}(10)L$.

Within this detectable window, the spectral morphol-

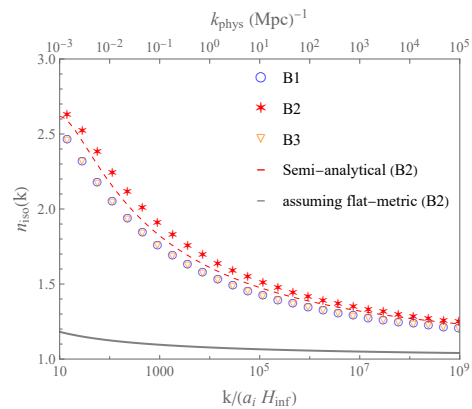


FIG. 4. Isocurvature spectral index $n_{\text{iso}}(k)$ inferred from the numerical spectra. The red dashed curve shows the semi-analytic estimate in Eq. (21) for B2. The gray curve indicates the corresponding flat-metric expectation.

ogy is controlled by radial dynamics. If the radial mode is strongly overdamped, $m_R^2 \lesssim \mathcal{O}(0.01)H_{\text{inf}}^2$, its evolution over the observable e-folds is negligible. For $R/L \lesssim \mathcal{O}(10)$, $m_\psi^2 \lesssim \mathcal{O}(0.1)H_{\text{inf}}^2$, yielding an approximately scale-invariant spectrum with negligible running. Such a signal may remain detectable at CMB scales but does not generate distinctive small-scale structure. In contrast, for mild slow-roll with $m_R^2 \lesssim \mathcal{O}(0.1)H_{\text{inf}}^2$, the radial field evolves by order unity and the geometry-induced mass satisfies $m_\psi^2 \sim H_{\text{inf}}^2$. The resulting axion isocurvature spectrum is then significantly blue-tilted, suppressed on CMB scales yet enhanced on small scales, with potentially observable small-scale consequences. The same radial evolution also induces measurable running, providing a characteristic signature of the geometric mechanism.

The benchmarks are therefore chosen with $R/L \sim 10$ such that Δ_S^2 at CMB scales lies safely below current bounds, while smaller scales can be enhanced (with isocurvature-to-adiabatic ratio $\sim \mathcal{O}(1)$ near $k \sim 0.1 \text{Mpc}^{-1}$, consistent with current limits [11, 12, 45]).

The above result highlight that hyperbolic geometry can reopen parameter space that is excluded in the flat-metric case. In our benchmarks, we focussed on $H_{\text{inf}} = 10^{13}$ GeV and $f_a \sim 10^{14}-10^{16}$ GeV, as it lies near current upper limits and is the most constrained regime for isocurvature. In contrast, for $f(R) = R$, satisfying the CMB bound at $H_{\text{inf}} = 10^{13}$ GeV typically requires extreme radial excursion ($R_i/f_a \sim 10^4-10^5$), implying super-Planckian displacements.

Fig. 4 shows the isocurvature tilt and its running inferred from numerical spectra shown in Fig. 3. When $m_\psi^2/H_{\text{inf}}^2$ varies slowly around horizon exit, the tilt is well approximated by the massive-mode estimate

$$n_{\text{iso}}(k) \simeq 4 - 2\sqrt{\frac{9}{4} - \frac{m_\psi^2(t(k))}{H_{\text{inf}}^2}}, \quad (21)$$

with $t(k)$ fixed by $k = a(t)H_{\text{inf}}$. Evaluating $m_\psi^2(t)$ using the numerical solution and substituting into Eq. (21)

reproduces the approximate $n_{\text{iso}}(k)$ as shown by the red dashed curve in Fig. 4 for B2.

In the slow-roll geometric domain, the hyperbolic metric ties the axial mass to the radial background through $\xi \equiv R/L$. For quartic PQ slow-roll, we give the following scale-dependent mass template (see App. B)

$$m_\psi^2(k > k_m) \simeq m_\psi^2(k_m) \left[1 + \frac{2}{3} \left(\frac{m_\psi^2(k_m)}{H_{\text{inf}}^2 \xi_m} \right) \ln \left(\frac{k}{k_m} \right) \right]^{-3/2}, \quad (22)$$

where k_m is a matching scale at the onset of the geometric regime and $\xi_m \equiv R_m/L$ controls the shape. For the benchmark scenarios, a convenient prescription is to fix k_m by $n_{\text{iso}}(k_m) = 2$, equivalently $m_\psi^2(k_m)/H_{\text{inf}}^2 = 5/4$, so that for $k \gtrsim k_m$ the entire running is governed by the single parameter ξ_m , labelling the family of trajectories.

The salient point is the functional form. In the hyperbolic regime one has $m_\psi^2 \propto \xi m_R^2 \propto R m_R^2$, and for a quartic slow-roll trajectory this gives

$$m_\psi^2(N) \propto (N - N_m)^{-3/2} \leftrightarrow m_\psi^2(k) \propto \left[\ln \left(\frac{k}{k_m} \right) \right]^{-3/2}. \quad (23)$$

This is steeper than the familiar $(N - N_m)^{-1}$ scaling that arises for a broad class of slow-roll backgrounds (e.g. monomial potentials) [46]. The extra half-power is the geometric fingerprint and arises from the hyperbolic lever arm contributing an additional factor of R to the canonical effective mass m_ψ^2 . Thus, the scale-dependence is well captured by Eqs. (21) and (22) which define a predictive template in which the running directly measures the field-space curvature through ξ_m . Fitting the numerical spectral-tilts in Fig. 4 with our template gives $\xi_m \simeq 12$ for B1, B3 and $\xi_m \simeq 14.5$ for B2, consistent with the benchmark values, and explains the apparent similarity of the isocurvature spectral shapes in Fig. 3.

V. CONCLUSION

We have demonstrated that the intrinsic geometry of the PQ field manifold provides a minimal and symmetry-preserving solution for the axion isocurvature problem. The curved (hyperbolic) field-space enhances the effective decay constant and can suppress CMB-scale isocurvature. The angular fluctuation acquires a geometric, time-dependent effective mass during inflation, without any explicit PQ breaking in the axion potential.

The phenomenology is governed by the geometric lever arm R/L and radial dynamics. For moderate $R/L \lesssim \mathcal{O}(10)$, the signal can remain detectable and CMB-compatible while radial slow-roll enhances small-scale power and induces measurable running. If the radial mode is strongly overdamped, the spectrum is nearly scale-invariant with negligible running, whereas very large R/L suppresses the signal altogether. In benchmark realizations with $H_{\text{inf}} = 10^{13}$ GeV, this mechanism reopens parameter space at large f_a that is typically excluded in flat field-space.

Beyond enlarging the viable QCD-axion window at high inflationary scales, our results highlight that isocurvature scale-dependence can directly probe field-space curvature. We provided a compact template linking the running of the isocurvature tilt to a single curvature-controlled parameter, enabling model-agnostic tests of the mechanism and straightforward incorporation into future analyses.

Several broad directions are motivated by this perspective. On the theory side, constructing controlled UV realizations of hyperbolic metrics in PQ models, and extending the framework to more general target spaces (e.g. non-constant curvature or non-diagonal metrics) are important. On the dynamics side, nontrivial background motion such as $\dot{\theta} \neq 0$ or post-inflationary evolution may introduce additional observational constraints, or signatures beyond the power spectrum [47, 48]. Within rotating-field mechanisms such as Affleck-Dine dynamics in baryogenesis ([49]), axiogenesis [50] and kinetic-misalignment in [51], hyperbolic geometry can support large angular velocities. Finally, the predicted enhancement of sub-CMB power motivates systematic confrontation with small-scale probes, including Lyman- α [45], UV luminosity functions [52], 21-cm measurements [53], and strong-lensing substructure [54, 55], offering a direct observational window onto PQ field-space geometry.

ACKNOWLEDGMENTS

We thank Peter Graham, Davide Racco, Raymond Co, and Tomo Takahashi for helpful comments and correspondence.

END MATTER

Appendix A: An example of hyperbolic PQ field-space

In our setup the PQ sector is described by a single complex scalar Φ . At the level of a low-energy effective theory, the most general two-derivative kinetic term takes the form of a nonlinear sigma model,

$$\mathcal{L}_{\text{kin}} = \frac{1}{2} g_{ab}(\phi) \partial_\mu \phi^a \partial^\mu \phi^b, \quad (A1)$$

where ϕ^a are the two real components of Φ . The PQ symmetry is realized as a $U(1)$ isometry of the target space (shifts of the angular coordinate). We now give a concrete example showing how a hyperbolic geometry can arise.

In $\mathcal{N} = 1$ supergravity, scalar fields parameterize a Kähler manifold with metric ([56])

$$K_{i\bar{j}} = \frac{\partial^2 K}{\partial \phi^i \partial \bar{\phi}^{\bar{j}}}, \quad (A2)$$

and kinetic term

$$\mathcal{L}_{\text{kin}} = K_{i\bar{j}} \partial_\mu \phi^i \partial^\mu \bar{\phi}^{\bar{j}}. \quad (\text{A3})$$

Appropriate choices of the Kähler potential K generate hyperbolic metrics already for a single complex field. A canonical example (familiar from α -attractor models [57, 58]) is the “disk” Kähler potential

$$K(Z, \bar{Z}) = -3\alpha M_P^2 \ln\left(1 - \frac{|Z|^2}{3M_P^2}\right), \quad (\text{A4})$$

which yields the $SU(1,1)/U(1)$ -invariant Kähler geometry.

For (A4) one finds

$$K_{Z\bar{Z}} = \frac{\alpha}{(1 - |Z|^2/(3M_P^2))^2}. \quad (\text{A5})$$

Parametrizing the complex field as $Z = \rho e^{i\theta}$, the kinetic term is

$$\mathcal{L}_{\text{kin}} = \frac{\alpha}{(1 - \rho^2/(3M_P^2))^2} [(\partial\rho)^2 + \rho^2(\partial\theta)^2]. \quad (\text{A6})$$

Matching to the sigma-model normalization $\mathcal{L}_{\text{kin}} = \frac{1}{2} d\sigma^2$ gives $g_{\rho\rho} = 2K_{Z\bar{Z}}$ and $g_{\theta\theta} = 2K_{Z\bar{Z}}\rho^2$. Defining the canonically normalized radial field R by

$$\frac{dR}{d\rho} = \sqrt{2K_{Z\bar{Z}}} = \frac{\sqrt{2\alpha}}{1 - \rho^2/(3M_P^2)}, \quad (\text{A7})$$

one obtains

$$R = \sqrt{6\alpha} M_P \tanh^{-1}\left(\frac{\rho}{\sqrt{3} M_P}\right). \quad (\text{A8})$$

Substituting back into (A6) yields the hyperbolic line element

$$d\sigma^2 = dR^2 + L^2 \sinh^2\left(\frac{R}{L}\right) d\theta^2, \quad L = \sqrt{\frac{3\alpha}{2}} M_P. \quad (\text{A9})$$

Note that R is unbounded, $R \in [0, \infty)$, so the regime $R \gg L$ is readily accessible. The coordinate bound $\rho < \sqrt{3} M_P$ corresponds to the disk boundary lying at infinite geodesic distance in field-space, i.e. it is a coordinate artifact rather than a physical restriction.

We do not assume a complete supersymmetric completion in our analysis; however, this example illustrates that a PQ-like complex scalar with hyperbolic field space arises naturally in $\mathcal{N} = 1$ supergravity, with the target-space metric directly given by a well-motivated Kähler potential (and close cousins appearing widely in inflationary model building).

Appendix B: Semi-analytic template for the tilt and its running

Here we sketch the derivation of the scale-space template used in the main text. We work in the slow-roll geometric regime $\delta \equiv \xi(m_R/H)^2 \lesssim 1$ (where $H \simeq H_{\text{inf}}$ is approximately constant) and take the potential to be quartic over the relevant field range.

a. Geometric regime. From Eq. (16) (or Eq. (15) in the $R \gtrsim L$ limit), the dominant contribution to the canonically normalized angular mass is

$$m_\psi^2 \simeq \xi m_R^2, \quad \xi \equiv \frac{R}{L}, \quad m_R^2 \equiv \frac{V_{,R}}{R}, \quad (\text{B1})$$

where we neglect the subleading negative-curvature term $\propto -\dot{R}^2$ in the slow-roll limit.

b. Slow-roll background and N -scaling. For quartic slow-roll, $V_{,R} \simeq \lambda R^3$ and

$$3H\dot{R} \simeq -V_{,R} \simeq -\lambda R^3. \quad (\text{B2})$$

In terms of e-folds $N \equiv \ln a$ (so $dN = H dt$), this gives

$$\frac{dR}{dN} \simeq -\frac{\lambda}{3H^2} R^3 \quad \Rightarrow \quad \frac{1}{R^2(N)} = \frac{1}{R_m^2} + \frac{2\lambda}{3H^2} (N - N_m), \quad (\text{B3})$$

where N_m is a reference e-fold at which we match onto the geometric regime and $R_m \equiv R(N_m)$. Using $m_R^2 = \lambda R^2$ and $\xi = R/L$, Eq. (B1) implies

$$m_\psi^2(N) \simeq \frac{\lambda}{L} R^3(N). \quad (\text{B4})$$

Combining with Eq. (B3) yields the characteristic falloff

$$m_\psi^2(N) \simeq m_{\psi,m}^2 \left[1 + \frac{2}{3} \left(\frac{m_{\psi,m}^2}{H^2 \xi_m} \right) (N - N_m) \right]^{-3/2}, \quad (\text{B5})$$

where $m_{\psi,m}^2 \equiv m_\psi^2(N_m)$ and $\xi_m \equiv R_m/L$. (The identity used above is $m_{\psi,m}^2/H^2 = \xi_m m_{R,m}^2/H^2$.)

c. k -space template. For nearly constant H , horizon exit implies $k = aH$ and hence

$$\ln\left(\frac{k}{k_m}\right) \simeq N - N_m, \quad (\text{B6})$$

with $k_m \equiv a(N_m)H$. Substituting Eq. (B6) into Eq. (B5) gives Eq. (22) in the main text,

$$m_\psi^2(k) \simeq m_\psi^2(k_m) \left[1 + \frac{2}{3} \left(\frac{m_\psi^2(k_m)}{H^2 \xi_m} \right) \ln\left(\frac{k}{k_m}\right) \right]^{-3/2}. \quad (\text{B7})$$

Together with the massive-mode estimate (21), this yields a unique analytic template for the tilt and its running for modes exiting after matching, $k \gtrsim k_m$.

d. Choice of matching scale. A convenient prescription is to define k_m by a fixed tilt value,

$$n_{\text{iso}}(k_m) = 2, \quad (\text{B8})$$

which using Eq. (21) is equivalent to $m_\psi^2(k_m)/H^2 = 5/4$. With this choice, the subsequent scale-dependence for $k \gtrsim k_m$ is controlled by the single curvature parameter ξ_m .

In the geometric slow-roll regime one obtains for $k \gtrsim k_m$,

$$m_{\psi}^2(N) \propto (N - N_m)^{-3/2} \leftrightarrow m_{\psi}^2(k) \propto \left[\ln \left(\frac{k}{k_m} \right) \right]^{-3/2}, \quad (\text{B9})$$

which is the origin of the characteristic non-power-law running emphasized in the main text.

-
- [1] R. D. Peccei and H. R. Quinn, CP Conservation in the Presence of Instantons, *Phys. Rev. Lett.* **38**, 1440 (1977).
- [2] R. D. Peccei and H. R. Quinn, Constraints Imposed by CP Conservation in the Presence of Instantons, *Phys. Rev. D* **16**, 1791 (1977).
- [3] S. Weinberg, A New Light Boson?, *Phys. Rev. Lett.* **40**, 223 (1978).
- [4] F. Wilczek, Problem of Strong P and T Invariance in the Presence of Instantons, *Phys. Rev. Lett.* **40**, 279 (1978).
- [5] D. J. E. Marsh, Axion Cosmology, *Phys. Rept.* **643**, 1 (2016), arXiv:1510.07633 [astro-ph.CO].
- [6] L. Di Luzio, M. Giannotti, E. Nardi, and L. Visinelli, The landscape of QCD axion models, *Phys. Rept.* **870**, 1 (2020), arXiv:2003.01100 [hep-ph].
- [7] J. Preskill, M. B. Wise, and F. Wilczek, Cosmology of the Invisible Axion, *Phys. Lett. B* **120**, 127 (1983).
- [8] L. F. Abbott and P. Sikivie, A Cosmological Bound on the Invisible Axion, *Phys. Lett. B* **120**, 133 (1983).
- [9] M. Dine and W. Fischler, The Not So Harmless Axion, *Phys. Lett. B* **120**, 137 (1983).
- [10] M. Badziak and K. Harigaya, Naturally astrophobic QCD axion, *JHEP* **06**, 014, arXiv:2301.09647 [hep-ph].
- [11] D. J. H. Chung and A. Upadhye, Search for strongly blue axion isocurvature, *Phys. Rev. D* **98**, 023525 (2018), arXiv:1711.06736 [astro-ph.CO].
- [12] Y. Akrami *et al.* (Planck), Planck 2018 results. X. Constraints on inflation, *Astron. Astrophys.* **641**, A10 (2020), arXiv:1807.06211 [astro-ph.CO].
- [13] E. Calabrese *et al.* (Atacama Cosmology Telescope), The Atacama Cosmology Telescope: DR6 constraints on extended cosmological models, *JCAP* **11**, 063, arXiv:2503.14454 [astro-ph.CO].
- [14] M. P. Hertzberg, M. Tegmark, and F. Wilczek, Axion Cosmology and the Energy Scale of Inflation, *Phys. Rev. D* **78**, 083507 (2008), arXiv:0807.1726 [astro-ph].
- [15] T. Higaki, K. S. Jeong, and F. Takahashi, Solving the Tension between High-Scale Inflation and Axion Isocurvature Perturbations, *Phys. Lett. B* **734**, 21 (2014), arXiv:1403.4186 [hep-ph].
- [16] K. Choi, E. J. Chun, S. H. Im, and K. S. Jeong, Diluting the inflationary axion fluctuation by a stronger QCD in the early Universe, *Phys. Lett. B* **750**, 26 (2015), arXiv:1505.00306 [hep-ph].
- [17] R. T. Co, E. Gonzalez, and K. Harigaya, Axion Misalignment Driven to the Bottom, *JHEP* **05**, 162, arXiv:1812.11186 [hep-ph].
- [18] L. Heurtier, F. Huang, and T. M. P. Tait, Resurrecting low-mass axion dark matter via a dynamical QCD scale, *JHEP* **12**, 216, arXiv:2104.13390 [hep-ph].
- [19] M. Berbig, Minimal solution to the axion isocurvature problem from nonminimal coupling, *Phys. Rev. D* **110**, 095008 (2024), arXiv:2404.06441 [hep-ph].
- [20] P. Chakraborty, J. Cheng, M. Reece, and Z. Wang, A Step in Flux to Suppress Axion Isocurvature, (2025), arXiv:2507.12519 [hep-ph].
- [21] J. Kearney, N. Orlofsky, and A. Pierce, High-Scale Axions without Isocurvature from Inflationary Dynamics, *Phys. Rev. D* **93**, 095026 (2016), arXiv:1601.03049 [hep-ph].
- [22] M. Kamionkowski and J. March-Russell, Planck scale physics and the Peccei-Quinn mechanism, *Phys. Lett. B* **282**, 137 (1992), arXiv:hep-th/9202003.
- [23] S. M. Barr and D. Seckel, Planck scale corrections to axion models, *Phys. Rev. D* **46**, 539 (1992).
- [24] S. Kasuya, M. Kawasaki, and T. Yanagida, Cosmological axion problem in chaotic inflationary universe, *Phys. Lett. B* **409**, 94 (1997), arXiv:hep-ph/9608405.
- [25] S. Kasuya, M. Kawasaki, and T. Yanagida, Domain wall problem of axion and isocurvature fluctuations in chaotic inflation models, *Phys. Lett. B* **415**, 117 (1997), arXiv:hep-ph/9709202.
- [26] M. Kawasaki, T. T. Yanagida, and K. Yoshino, Domain wall and isocurvature perturbation problems in axion models, *JCAP* **11**, 030, arXiv:1305.5338 [hep-ph].
- [27] E. J. Chun, Axion Dark Matter with High-Scale Inflation, *Phys. Lett. B* **735**, 164 (2014), arXiv:1404.4284 [hep-ph].
- [28] K. Nakayama and M. Takimoto, Higgs inflation and suppression of axion isocurvature perturbation, *Phys. Lett. B* **748**, 108 (2015), arXiv:1505.02119 [hep-ph].
- [29] K. Harigaya, M. Ibe, M. Kawasaki, and T. T. Yanagida, Dynamics of Peccei-Quinn Breaking Field after Inflation and Axion Isocurvature Perturbations, *JCAP* **11**, 003, arXiv:1507.00119 [hep-ph].
- [30] T. Kobayashi and F. Takahashi, Cosmological Perturbations of Axion with a Dynamical Decay Constant, *JCAP* **08**, 056, arXiv:1607.04294 [hep-ph].
- [31] I. J. Allali, M. P. Hertzberg, and Y. Lyu, Altered axion abundance from a dynamical Peccei-Quinn scale, *Phys. Rev. D* **105**, 123517 (2022), arXiv:2203.15817 [hep-ph].
- [32] M. Fairbairn, R. Hogan, and D. J. E. Marsh, Unifying inflation and dark matter with the Peccei-Quinn field: observable axions and observable tensors, *Phys. Rev. D* **91**, 023509 (2015), arXiv:1410.1752 [hep-ph].
- [33] P. W. Graham and D. Racco, Revisiting isocurvature bounds on the minimal QCD axion, *JHEP* **12**, 028, arXiv:2506.03348 [hep-ph].
- [34] S. Kasuya and M. Kawasaki, Axion isocurvature fluctuations with extremely blue spectrum, *Phys. Rev. D* **80**, 023516 (2009), arXiv:0904.3800 [astro-ph.CO].
- [35] D. J. H. Chung and H. Yoo, Elementary Theorems Regarding Blue Isocurvature Perturbations, *Phys. Rev. D* **91**, 083530 (2015), arXiv:1501.05618 [astro-ph.CO].
- [36] D. J. H. Chung and S. C. Tadepalli, Large blue spectral index from a conformal limit of a rotating complex scalar, *Phys. Rev. D* **111**, 083527 (2025), arXiv:2406.12976 [astro-ph.CO].
- [37] A. R. Brown, Hyperbolic Inflation, *Phys. Rev. Lett.* **121**, 251601 (2018), arXiv:1705.03023 [hep-th].
- [38] S. Mizuno and S. Mukohyama, Primordial perturbations

- from inflation with a hyperbolic field-space, *Phys. Rev. D* **96**, 103533 (2017), arXiv:1707.05125 [hep-th].
- [39] C.-B. Chen and J. Soda, Geometric structure of multi-form-field isotropic inflation and primordial fluctuations, *JCAP* **05** (05), 029, arXiv:2201.03160 [hep-th].
- [40] L. Iacconi and D. J. Mulryne, Multi-field inflation with large scalar fluctuations: non-Gaussianity and perturbativity, *JCAP* **09**, 033, arXiv:2304.14260 [astro-ph.CO].
- [41] M. De Angelis and C. van de Bruck, Adiabatic and isocurvature perturbations in extended theories with kinetic couplings, *JCAP* **10**, 023, arXiv:2304.12364 [hep-th].
- [42] H. M. Lee, A. G. Menkara, M.-J. Seong, and J.-H. Song, Inflation models with Peccei–Quinn symmetry and axion kinetic misalignment, *Eur. Phys. J. C* **84**, 1260 (2024), arXiv:2408.17013 [hep-ph].
- [43] G. Grilli di Cortona, E. Hardy, J. Pardo Vega, and G. Villadoro, The QCD axion, precisely, *JHEP* **01**, 034, arXiv:1511.02867 [hep-ph].
- [44] T. Sai Chaitanya, Supplemental Material: Axions on a Hyperbolic Ride: Geometric Suppression of CMB Isocurvature and a Blue-Tilted Spectrum.
- [45] M. R. Buckley, P. Du, N. Fernandez, and M. J. Weikert, General constraints on isocurvature from the CMB and Ly- α forest, *JCAP* **12**, 006, arXiv:2502.20434 [astro-ph.CO].
- [46] D. H. Lyth and A. Riotto, Particle physics models of inflation and the cosmological density perturbation, *Phys. Rept.* **314**, 1 (1999), arXiv:hep-ph/9807278.
- [47] S. Renaux-Petel, Inflation with strongly non-geodesic motion: theoretical motivations and observational imprints, *PoS EPS-HEP2021*, 128 (2022), arXiv:2111.00989 [astro-ph.CO].
- [48] H. Firouzjahi, M. A. Gorji, S. Mukohyama, and A. Talebian, Dark matter from entropy perturbations in curved field space, *Phys. Rev. D* **105**, 043501 (2022), arXiv:2110.09538 [gr-qc].
- [49] I. Affleck and M. Dine, A new mechanism for baryogenesis, *Nuclear Physics B* **249**, 361 (1985).
- [50] R. T. Co and K. Harigaya, Axiogenesis, *Phys. Rev. Lett.* **124**, 111602 (2020), arXiv:1910.02080 [hep-ph].
- [51] R. T. Co, L. J. Hall, and K. Harigaya, Axion Kinetic Misalignment Mechanism, *Phys. Rev. Lett.* **124**, 251802 (2020), arXiv:1910.14152 [hep-ph].
- [52] S. Yoshiura, M. Oguri, K. Takahashi, and T. Takahashi, Constraints on primordial power spectrum from galaxy luminosity functions, *Phys. Rev. D* **102**, 083515 (2020), arXiv:2007.14695 [astro-ph.CO].
- [53] T. Minoda, S. Yoshiura, and T. Takahashi, Probing isocurvature perturbations with 21-cm global signal in the light of HERA result, *Phys. Rev. D* **105**, 083523 (2022), arXiv:2112.15135 [astro-ph.CO].
- [54] N. Dalal and C. S. Kochanek, Strong lensing constraints on small scale linear power, (2002), arXiv:astro-ph/0202290.
- [55] J. Wu, T. K. Chan, and V. J. F. Moreno, Cosmological zoom-in simulations of Milky Way host mass dark matter halos with a blue-tilted primordial power spectrum, *Phys. Rev. D* **112**, 023512 (2025), arXiv:2412.16072 [astro-ph.CO].
- [56] J. Wess and J. Bagger, *Supersymmetry and supergravity* (Princeton University Press, Princeton, NJ, USA, 1992).
- [57] J. J. M. Carrasco, R. Kallosh, and A. Linde, Cosmological Attractors and Initial Conditions for Inflation, *Phys. Rev. D* **92**, 063519 (2015), arXiv:1506.00936 [hep-th].
- [58] J. J. M. Carrasco, R. Kallosh, A. Linde, and D. Roest, Hyperbolic geometry of cosmological attractors, *Phys. Rev. D* **92**, 041301 (2015), arXiv:1504.05557 [hep-th].